Guided transport of hot electrons in solid using magnetic field induced by resistivity gradient

S. Kar, K. Markey and M. Zepf

School of Mathematics and Physics, Queen's University of Belfast, Belfast BT7 1NN, UK

Contact | **m.zepf@qub.ac.uk**

A. P. L. Robinson and D. Neely

Central Laser Facility, STFC, Rutherford Appleton Laboratory, HSIC, Didcot, Oxon OX11 0QX, UK

D. C. Carroll and P. McKenna

Department of Physics, University of Strathclyde, Glasgow G4 0NG, UK

Introduction

Achieving collimated transport of fast electrons through solid density plasmas is a hot topic because of its relevance for fast ignition (FI), high energy density physics, laser induced radiation sources and particle acceleration. Experimental studies, via laser and target parameter scans, on hot electron transport in solids show minimum spray angles of 30-40°[1] – which limits the efficiency with which energy can be coupled to the hot spot in FI. Therefore various schemes are being investigated to achieve less divergent or even collimated transport. In addition to the ideas such as cone[2] and wire[3] guiding, recent theoretical studies proposed a concept based on self-generated magnetic fields at resistivity boundaries[4]. According to Maxwell's equations a resistivity gradient with the same sign as the electron current density gradient will lead to the generation of a magnetic field (due to the $\nabla\eta\times J$ term in the Faraday's law, where η is the resistivity and J is the current density). Once established, this field is further enhanced by magnetic field due to the current density gradient (the term $\nabla\eta\times J$ in the Faraday's law). Simulations have shown that for the parameters of the Vulcan PW, the field strength is sufficient to collimated an MeV electron beam. For experiments with initially cold targets, it is essential to maintain the sign of the resistivity gradient across the Z-boundary as the target heats up to hundreds of eV during the interaction. Here this is achieved by using a core material (in which the electron beam is confined) with a higher Z and higher initial core resistivity than the surrounding medium. We report here on the first experimental campaign investigating the scheme by fielding targets with parallel Z-boundary (an one dimensional analogy of the scheme – a first and straightforward step to test the concept experimentally), as shown in the figure 1(a). The results show stronger collimation of the fast electrons within the Z-boundaries than along the sandwiched high Z layer.
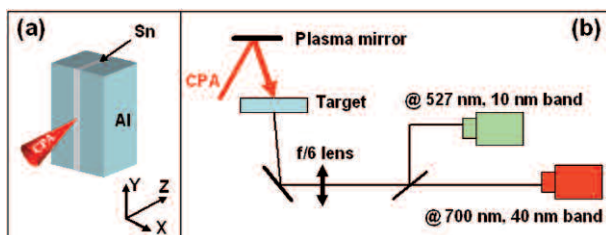

Figure 1. Schematic of the (a) Al-Sn-Al sandwich target employed in the experiment and (b) experimental setup.

Experimental setup

The experiment was performed at Rutherford Appleton Laboratory employing Vulcan Petawatt laser system. After reflection from a plasma mirror, the laser pulse delivered ~150 J of energy on target in *fwhm* duration of 1 ps. Laser spot size on the target was 20 μm, reaching peak intensity of ~10^{20} W/cm^2 on target at near normal incidence. The one dimensional electron guiding target fielded in the experiment is shown schematically in figure 1(a). The CPA was targeted to irradiate the embedded 12.5 μm thick Tin (Sn) layer sandwiched between two Aluminium (Al) slabs. The materials were chosen based on the contrast of their atomic weights and electrical resistivities, as well from the point of view of fabrication. The ratio between atomic numbers and cold electrical resitivities of Sn and Al are 4:1 and 4.5:1 respectively. The thickness of the target along the laser propagation direction was 200μm. The target rear surface was lapped to a roughness of ~50 nm rms and was gold coated (of sub micron thickness). Optical emission from the target rear surface were collected by f/6 imaging. Time integrated images of the rear surface emission at 527±5 nm and 700±20 nm wavelengths (using bandpass optical filters) were simultaneously recorded by separate CCD cameras. The spatial resolution of the images at 527 nm and 700 nm were 4 μm and 5.5 μm respectively.

Results

Figure 2(a) shows the time integrated image of the optical emission from the Al-Sn-Al target rear surface at 527 nm. It is striking to see the oblong shape, width and the orientation of the image in the experimental data which correlates well with the Tin layer of the guiding target fielded in the experiment. The oblong shape of the image with its major axis along the sandwiched tin layer contrasts with the approximately circular symmetry obtained from the reference 200 μm thick Al target (not shown here, examples can be found in press[5,6]. In figure 2(a) the central bright spot (labeled as 'A') is having major to minor axes ratio ~2.5:1, and, the *fwhm* of the minor axis is close to the thickness of the sandwiched tin layer (see figure 2(c)). Comparison of the lineout shows that the intensity distribution along the Sn plane is far more peaked than the electron distribution in the simulations, while the overall extent is similar. Note however, that the 527 nm light is due to Optical Transition Radiation (OTR) at $2\omega_{laser}$[7]. OTR is proportional not to the total electron number, but to the square of the Fourier transform of the
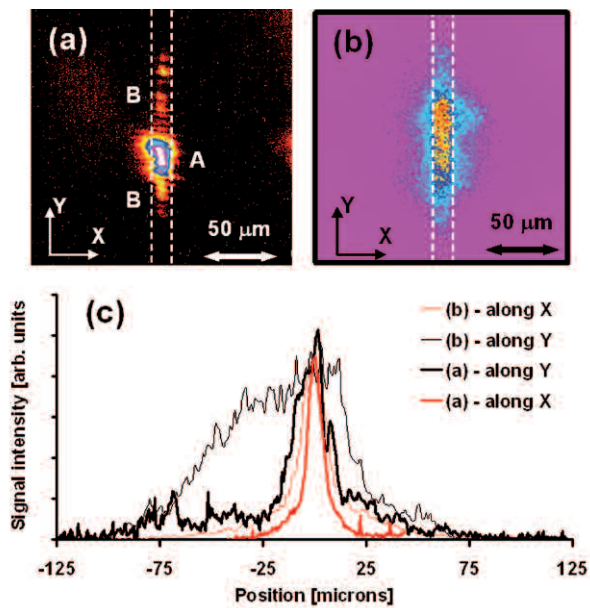
Figure 2 (a). Experimentally obtained time integrated image of optical transition radiation from the Al-Sn-Al target rear surface at 527 nm. Labels 'A' and 'B' represent respectively the central bright spot and the dim line feature (along Y) on both sides of 'A'. (b) 2D spatial distribution of square of the hot electron density at the rear surface of the modelled sandwich target obtained from 3D hybrid code. The square of electron density profile at z=200 μm is considered for a direct comparison with the narrow band coherent transition radiation at twice the laser frequency [5], shown in (a). Dotted white lines in (a) and (b) show the tentative position and width of the sandwiched Sn layer of the target. (c) Graph showing the comparison between lineout of (a) (thick line) and (b) (thin line) along X (red) and Y (black) directions.

electron density. Consequently, the OTR images at 527nm measure the density of electrons bunched at $2\omega_{laser}$. Consequently the more rapid fall off in intensity may be due to increased debunching of the off-axis electrons due to the collimating fields.

Nevertheless, the overall size of the OTR signal in both axes is well reproduced by the simulation, as shown in the figure 2(c). The simulation was carried out modeling the 1D geometry, employing the 3D hybrid code ZEPHYROS[4]. The simulation box was 200×200×200 μm in dimension with the cell size being 1×1×1μm. Fast electrons were injected from the z = 0 plane with the injection region being centered on x = y = 100 μm. The transverse electron distribution and fast electron temperature was determined from the scaling laws [8] for the current experimental parameters. This heating profile was constant over the laser pulse duration which was set to 500 fs. The electrons were injected uniformly over a solid angle of 60°. Roughly 26000 quasi-particles were injected per time step, which is 5 quasi-particles per injection cell per time step. The resistivities of the materials (i.e. Al and Sn) were modeled in the same way that Davies *et al.*[9] and using Spitzer theory for fully ionized metal at very high temperatures.

The specific heat capacities are determined by the same fit to the Thomas-Fermi model that Davies[9] uses. The simulations were run up to 1.5 ps. Reflective spatial boundaries were used throughout.

The reference simulation was carried out with a simulation box made of Al only. In case of the collimation target, the sandwiched Tin slab was of 12 μm thick centered at x=100 μm. As expected, the simulation for the Al target produced a fairly uniform electron distribution of ~100 μm fwhm at the rear surface (i.e. z =200 μm plane). On the other hand, the asymmetrical electron distribution obtained for the case of sandwich target can be seen in figure 2(b). Due to the resistivity gradient across the interfaces, the generated strong magnetic walls at the interfaces confine the electron within it, whereas some of the electrons managed to escape before the strength of the magnetic field could be sufficient to confine them. The magnetic field lines at the two interfaces joins together at the top and bottom (along Y axis) of the simulation box passing through the tin layer. This part of the magnetic field has a similar strength as that in the interfaces and inhibits the spreading of the electrons along the tin layer (Y axis). The simulation also reproduces the ratio between the number of electrons escaped to the number of electrons confined along the X axis (the collimation axis), thus establish the underlying dynamics of the magnetic field.
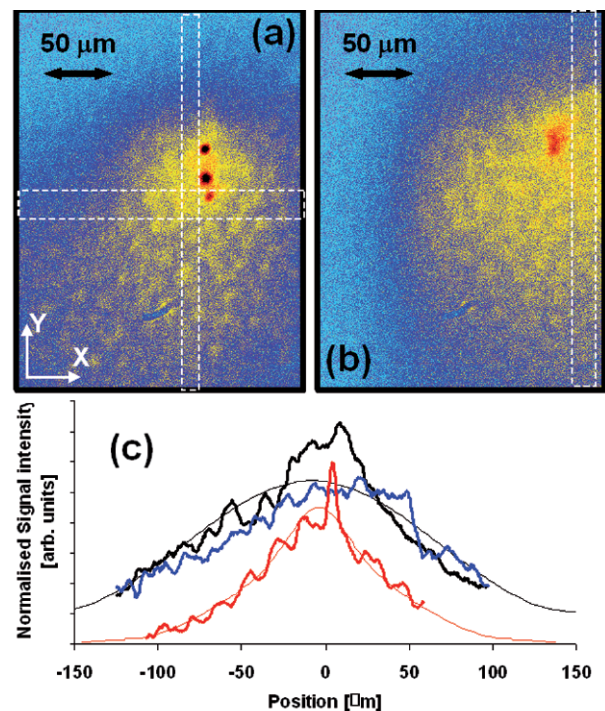

Figure 3. (a) and (b) are the time integrated image of the optical emission from the Al-Sn-Al target and pure Al reference target, respectively, rear surface at 700 nm wavelength. (c) Comparison between the box (as indicated by the white broken lines in (a) and (b)) lineout of (a) along X (thick red) and Y (thick black) axes, and of (b) along Y (thick blue) axis. The thin red and black lines are, respectively, the lineout along X and Y axes of the simulated thermal emission profile (not shown).

The experimentally obtained heating profile of the target rear surface provides further evidence of collimated electron flow. The difference between collimated flow and reference shot are not expected to be as marked as for the OTR, since thermal transport will tend to wash out these features in the infra-red. Howerver, a marked difference consistent with collimated transport is still visible. Figure 3(a) and (b) shows the images formed by thermal radiation from the rear surface of the sandwich target and reference Al target respectively. Figure 3a shows an elliptical whereas, the reference target produced a uniform and circular heating profile (see figure 3(b)). As shown in figure 3(c), the fwhm of the reference shot heating profile is same as the fwhm of the figure 3(a) along the Y axis. By contrast, the heated region fwhm of the reference shot is approximately twice of the fwhm along the collimating axis (X axis) observed from the Al-Sn-Al target.

We compared the experimentally obtained heating profile from the collimating target with the one obtained by post-processing the ZEPHYROS simulated temperature profile across the plane z=200 µm towards the end of the run. The post-processing of the simulated heating profile was done with the 2D hydrodynamic code POLLUX[10]. We simulated the transverse (across the target rear surface) spreading of the heated region for 3 ns with a temperature profile output at every 100 ps. For every time step, the emitted thermal radiation (in the range 700 ± 20 nm wavelength) from the surface is computed (spatially resolved) according to the Plank's law of blackbody radiation. The simulated time integrated thermal emission profile thus obtained has fwhm of 80 µm and 150 µm along X and Y axes respectively, in good agreement with the experimental data.

Conclusion

It has been experimentally demonstrated that collimated flow of hot electrons inside a solid density target can be achieved in targets with suitable resistivity gradients. The resistivity gradients at the interfaces are practically maintained, for the relevant time scale, by choosing central metal of higher atomic number as well as higher electrical resistivity than the surrounding one. The experimental data based on measurements of the target rear surface transition radiation and thermal emission are in good agreement with 3D hybrid simulations.

Acknowledgements

References

1. K. Lancaster *et al*., *Phys. Rev. Letts.,* **98**, 125002 (2007).
2. R. Kodama *et al*., *Nature*, **432**, 1005 (2004).
3. J. S. Green *et al*., *Nature Phys*., **3**, 853 (2007).
4. A. P. L. Robinson *et al*., *Phys. Plasmas*, **14**, 083105 (2007).
5. J. J. Santos *et al*., *Phys. Rev. Lett*., **89**, 025001 (2002).
6. H. Popescu *et al*., *Phys. Plasmas*, **12**, 063106 (2005).
7. S. D. Baton *et al*., *Phys. Rev. Lett*., **91**, 105001 (2003).
8. S. C. Wilks *et al*., *IEEE J. Quantum Electronics*, **33**, 1954 (2000).
9. J. Davis, *Phys. Rev. E*, **65**, 026407 (2002).
10. G. J. Pert, *J. Comp. Phys*., **43**(1), 111 (1981).